Global transcriptional reprogramming by cytomegalovirus infection suppresses antigen presentation while enhancing migration machinery in murine dendritic cells.

Rhys H. Parry[1,*,+], Christopher L. D. McMillan[1,2,+], Kimberley L. Bruce[1], Helen E. Farrell[1,2*]

[1]School of Chemistry and Molecular Biosciences, The University of Queensland, St Lucia, Queensland 4072, Australia

[2]Australian Infectious Diseases Research Centre, Brisbane, Queensland 4072, Australia

+These authors contributed equally.

*Correspondence:
Rhys H. Parry, r.parry@uq.edu.au; Helen E. Farrell, h.farrell1@uq.edu.au

ABSTRACT

Dendritic cells (DCs) serve dual roles in cytomegalovirus infection: orchestrating antiviral immunity and acting as vehicles for viral dissemination. DC-dependent systemic spread of mouse cytomegalovirus (MCMV) is dependent on expression of a viral G protein-coupled receptor (GPCR) homolog, encoded by M33. We performed global transcriptional profiling of murine DCs infected with either wild-type mouse MCMV or a M33 mutant harboring a single point mutation (R131Q; denoted M33NQY) which ablates constitutive G protein-dependent signalling. RNA-seq analysis revealed that MCMV induces substantial transcriptional reprogramming, with over 2,400 significantly altered genes affecting key immune and migration pathways. Wild-type MCMV infection resulted in 1,883 upregulated and 658 downregulated genes, while M33NQY infection showed comparable effects with 1,905 upregulated and 668 downregulated genes. Both viruses systematically downregulated the MHC class II antigen presentation machinery, with substantial suppression of H2 molecules, peptide-loading components (H2-DM), and the class II transactivator CIITA ($\log_2$FC > -6.4). Pathways analysis revealed coordinated disruption of B cell receptor signaling, leukocyte transendothelial migration, and antigen processing and presentation. A comparison between wild-type and M33NQY-infected DCs demonstrated that while both viruses similarly impair antigen presentation, M33 signaling specifically enhances the expression of genes involved in transendothelial migration, including Spp1 (osteopontin, $\log_2$FC = 0.65), cytoskeletal components (ACTG1, ACTB), adhesion molecules (ICAM1), and matrix interaction factors (Tnc, Plau). Network analysis identified critical hub genes, including B2m, Itgb1, Itgam, and Icam1 as key regulatory nodes connecting antigen presentation and migration pathways. This provides molecular evidence for a sophisticated viral strategy that shields MCMV from immune detection while hijacking DC migratory machinery to facilitate dissemination, with M33 serving as a specific enhancer of migration-related pathways.

Keywords: Cytomegalovirus, Dendritic cells, Leukocyte migration, MCMV, Transcriptome, Transendothelial migration, Immune evasion, Viral dissemination

INTRODUCTION

Dendritic cells (DCs) serve as sentinels of the immune system, initiating adaptive responses against pathogens while maintaining self-tolerance (Banchereau and Steinman, 1998; Merad et al., 2013). Strategically positioned at mucosal surfaces, DCs actively sample their environment to detect infection through pattern recognition receptors (Iwasaki, 2007). Upon pathogen encounter, DCs undergo morphological and functional changes, transitioning from a smooth, rounded state to an activated form characterized by extensive pseudopodia that facilitate their migration to draining lymph nodes (LN) (Randolph et al., 2005). This migration process is orchestrated by chemokine signaling networks that guide DCs through tissues via G protein-coupled chemokine (GPCR) receptor activation, leading to cytoskeletal reorganization and directional motility (Forster et al., 2008; Sozzani et al., 1998).

Within lymph nodes, migrated DCs localize to fibroblast reticular cell niches and position proximal to high endothelial venules (HEV) to facilitate interaction with incoming blood-borne T cells (Bajenoff et al., 2006; Sixt et al., 2005). In this context, mature DCs function as professional antigen-presenting cells (APCs), expressing pathogen-derived peptides via major histocompatibility complex (MHC) molecules and upregulating costimulatory signals that lower the threshold for T cell activation (Guermonprez et al., 2002; Reis e Sousa, 2006). Chemokines continue to shape DC behaviour throughout this process by engaging G protein-coupled chemokine receptors activating downstream pathways essential for DC chemotaxis, survival, cytokine production, and differentiation (Allavena et al., 2000). Importantly, these migratory APCs have a finite lifespan in lymph nodes, disappearing rapidly from T cell areas without entering efferent lymphatics—suggesting they undergo local elimination after fulfilling their immune activation role (Ingulli et al., 1997; Kamath et al., 2002; Garg et al., 2003).

Recent interrogations of the transcriptional DC landscape have revealed a multi-layered network of pathways that underpin the dynamic expression of DC stimulatory molecules during inflammation, particularly in response to virus challenge (Luber et al., 2010; Miller et al., 2012). These techniques provide a powerful approach to discover key checkpoints of host immunity that may be harnessed for clinical therapies. However, several persistent viruses also use DC as a vehicle to facilitate their dissemination, seemingly hijacking them to use as effective shields against host attack (Auffermann-Gretzinger et al., 2001). Their co-existence requires virus strategies to disrupt DC responses to extracellular inflammatory cues that may jeopardize both virus and host cell survival. The betaherpesvirus cytomegalovirus (CMV) is among this specialized virus group (Sinclair and Reeves, 2013).

Human CMV (HCMV) is a ubiquitous pathogen that causes a largely asymptomatic infection in immunocompetent hosts (Boeckh and Geballe, 2011). In persons whose immunity is immature or immunodeficient, HCMV has the propensity to cause disseminated lytic infection and inflammation, leading to severe morbidity or death (Griffiths et al., 2015). HCMV establishes a latent infection in $CD34^+$ hematopoietic myeloid progenitor cells and $CD14^+$ monocytes (Reeves and Sinclair, 2013; Sinclair and Sissons, 2006). Analysis of differentially expressed genes in latently infected $CD14^+$ monocytes showed marked downregulation in MHCII and CD74 transcripts, suggestive of HCMV interference in antigen presentation and endothelial transmigration functions (Shnayder et al., 2020; Yunis et al., 2018). In contrast, the role of DCs in facilitating primary HCMV spread is less clear, as infections are asymptomatic and thus difficult to capture and track. Given the difficulty in studying early HCMV dissemination, MCMV infection in mice offers a powerful alternative for dissecting virus-DC interactions *in vivo*.

Infection of mice with mouse cytomegalovirus (MCMV) has provided a tractable approach to track virus entry and spread (Bruce et al., 2022; Krmpotic et al., 2003). Naturally acquired MCMV exploits olfaction to enter new hosts, spreading from the olfactory epithelium to draining lymph nodes via infected DC (Farrell et al., 2016). Experimental lung inoculation of MCMV results in infection of alveolar/interstitial macrophages, type II alveolar epithelial cells and DC, with DCs remaining the principal vehicle for systemic spread (Bruce et al., 2022; Farrell et al., 2015). Remarkably, MCMV$^+$ DC are not retained in LN. Instead, they traverse to HEV, recirculate to the blood and extravasate across vascular endothelia to numerous tissues, including the salivary glands (Farrell et al., 2017; Ma et al., 2021). Indeed, lung infection of mice with a replication-deficient (i.e. single-cycle) MCMV results in translocation of MCMV$^+$ DC from the lungs to the salivary glands, detected seven days later. In the salivary glands, MCMV$^+$ DC transfer infection to acinar epithelial cells, where the virus is amplified, and extracellular virions are released in saliva (Farrell et al., 2017; Ma et al., 2021).

Consistent with the central role of host chemokines in DC trafficking, DC recirculation requires expression of MCMV chemokine receptor and chemokine homologs, which act in a non-redundant fashion at key stages of the DC journey (Saederup et al., 1999; Suvas and Rouse, 2006). In addition to MCMV-induced modifications in DC motility and directional decision-making, MCMV$^+$ DC exhibit other modifications, such as ablated responses to LN retention signals, diminished T cell engagement in LN, enhanced endothelial extravasation and enhanced DC survival (Andrews et al., 2001; Mathys et al., 2003). Many MCMV genes – some characterized already in other infected cell types- will likely contribute to the DC altered state. However, many described examples of MCMV-induced cellular dysregulation or immune evasion occur post-transcriptionally (Loewendorf and Benedict, 2010). Little is known about the global changes in the transcriptional landscape caused by MCMV infection of DC.

The viral GCPR (vGPCR) M33 plays a critical role in this process (Cardin et al., 2009; Davis-Poynter et al., 1997). DCs infected with MCMV lacking M33 (ΔM33) or expressing a signaling-deficient mutant (M33NQY) with a mutation in the vGPCR "DRY box motif" show markedly diminished ability to escape lymph nodes and enter the bloodstream (Farrell et al., 2017). This M33 signaling defect serves as a valuable tool to dissect M33-dependent functions throughout our study. While the phenotypic importance of M33 in DC-dependent viremia is established, the molecular mechanisms underlying this effect remain unknown. Similarly, MCMV-infected DCs exhibit altered immune functions, including reduced T cell engagement and enhanced survival, but the transcriptional basis for these changes has not been elucidated (Lemmermann et al., 2011).

In this study, we performed comprehensive transcriptional profiling of murine DCs infected with either wild-type MCMV or the signaling-deficient M33NQY mutant to identify the molecular pathways underlying viral manipulation of DC biology. We hypothesized that MCMV infection would induce coordinated transcriptional changes affecting both antigen presentation and migration pathways, with M33 specifically contributing to migration-related gene expression. Our findings reveal a sophisticated viral strategy that systematically targets the MHC class II antigen presentation machinery while selectively enhancing genes involved in trans endothelial migration, providing molecular insights into how MCMV exploits DCs for dissemination while evading immune detection.

MATERIALS AND METHODS

Cells and viruses.

The mouse Mutu DC line, which possesses a close resemblance to conventional DC was obtained from Michael Chopin, (Monash University, Australia) and were cultured in Iscove's Modified Dulbecco's Medium (IMDM; Gibco) supplemented with 10% heat-inactivated fetal calf serum (hiFCS), 2mM glutamine, 100 IU/mL penicillin, 100 µg/mL streptomycin and 50 µM 2-mercaptoethanol. DC were infected with a GFP-tagged MCMV (strain K181) diluted in IMDM containing 2% hiFCS when cultures were 75% confluent. Infections (n=3) were performed at a multiplicity of 5 and all cells were GFP+ within 24 h p.i. Following 1 h incubation with virus, cells were washed x 3 with IMDM containing no supplements, then incubated for a further 2 days in IMDM containing 2% hiFCS. Control cultures (n=3) were treated identically but without virus infection.

RNA isolation, library preparation and next-generation sequencing.

DC cultures (n=3 per group) were harvested two days after infection, and RNA was isolated using the RNeasy Mini Kit according to the Manufacturer's instructions (QIAGEN). RNA integrity was assessed with an Agilent Bioanalyzer 2100 system (Agilent Technologies) and RIN values ranged from 7-9. Stranded mRNA sequencing libraries were sequenced using the NextSeq 150 cycle kit (Illumina Inc) generating 75 bp paired-end reads. The Illumina bcl2fastq 2.20.0.422 pipeline was then used to produce the sequence data. The University of Queensland Genomics Facility and the Australian Genomics Research Facility (AGRF) performed library preparation, sequencing, and data acquisition. Image analysis was performed on the instrument computer using the HiSeq Control Software (HCS) vHD 3.4.0.38 and Real-Time Analysis (RTA) v2.7.7.

Transcriptome data analysis.

Raw, basecalled fastq files were first analysed using FastQC to assess read quality. FASTp (v0.24.0) was then used to eliminate adapters, low-quality reads, and reads below 50 bases. Remaining high-quality reads were mapped using HISAT2 (v2.2.1) to both Murine cytomegalovirus (strain K181) (Genbank ID: AM886412) and *Mus musculus* mm10 genome. Feature counts for genes were numerated using htseq-count (v0.9.1) under the conditions: union, stranded: yes, minimum alignment quality: 10, feature type: exon, and ID attribute: gene_ID using the GTF file mm10.refGene.gtf. Counts files were merged, and differential gene expression analysis was undertaken utilising edgeR (v3.36.0), setting min.total.count at 10 and employing estimateDisp() robust = TRUE as well as glmQLFTest() with a robust fit setting. Visualization of the fold change and P-value data was achieved through volcano plots generated using EnhancedVolcano (v1.12.0). Heatmaps were generated using the pheatmap R package (v1.0.12), with default normalization parameters where normalised expression values were scaled per gene to a z-score distribution.

Gene ontology and pathway enrichment analyses and Network reconstruction.

The entire differentially expressed gene set was subjected to pathway enrichment analysis using easyGSEA (Cheng et al., 2021). Multiple pathway databases were queried including Gene Ontology (Biological Process, Cellular Component, Molecular Function), KEGG, and Reactome pathways. Gene set filtering parameters were set to include only pathways containing between 15 and 200 genes. For gene set enrichment analysis (GSEA), 1,000 permutations were performed to establish statistical significance, and pathways with P-values < 0.005 were considered significantly enriched. For network reconstruction, leading edge DEGs from the

easyGSEA analysis specifically associated with Antigen Presentation and Leukocyte Migration pathways were extracted and imported into Cytoscape (v3.10.3). Protein-protein interaction (PPI) networks were constructed using stringApp (v2.2.0) with *Mus musculus* as the reference organism. Interactions were filtered using a confidence score threshold of > 0.4, and no additional interactors were included beyond the input gene set. The individual networks for Antigen Presentation and Leukocyte Migration were then integrated using Cytoscape's "merge networks" function with the "Union" mode to create a comprehensive interaction network. Network topology was analyzed by calculating betweenness centrality values for each node using Cytoscape's "Analyze Network" function, which quantifies the number of shortest paths passing through each node. To visualize differential expression within the network context, logFC values for each gene were incorporated as a node attribute and represented through a color gradient.

RESULTS

Global transcriptomic reprogramming of murine DCs in response to MCMV infection.

RNA sequencing of murine dendritic cells revealed extensive transcriptional reprogramming following infection with either wild-type MCMV (IC2) or the signaling-deficient M33NQY mutant. Mock-infected samples yielded an average of 16.9 million reads per library with high mapping efficiency to the mouse genome (97.26%). In contrast, both infected conditions showed a reduction in host reads due to viral transcription: IC2-infected samples contained 14.9 million reads (75.81% mapping to mouse genome, 18.46% to MCMV genome), while M33NQY-infected samples showed a similar distribution (14.1 million reads; 76.90% mouse, 17.15% MCMV) (Fig. 1A, Table S1). Despite these differences in raw mapping percentages, edgeR normalization effectively adjusted for these technical variations (Fig. 1B).

Multidimensional scaling analysis (Fig. 1C) demonstrated clear separation between infected and uninfected conditions along dimension 1 (capturing 94% of total variation), with dimension 2 (capturing 1% of variation) distinguishing between IC2 and M33NQY infections. Biological replicates within each condition clustered tightly together, confirming high reproducibility.

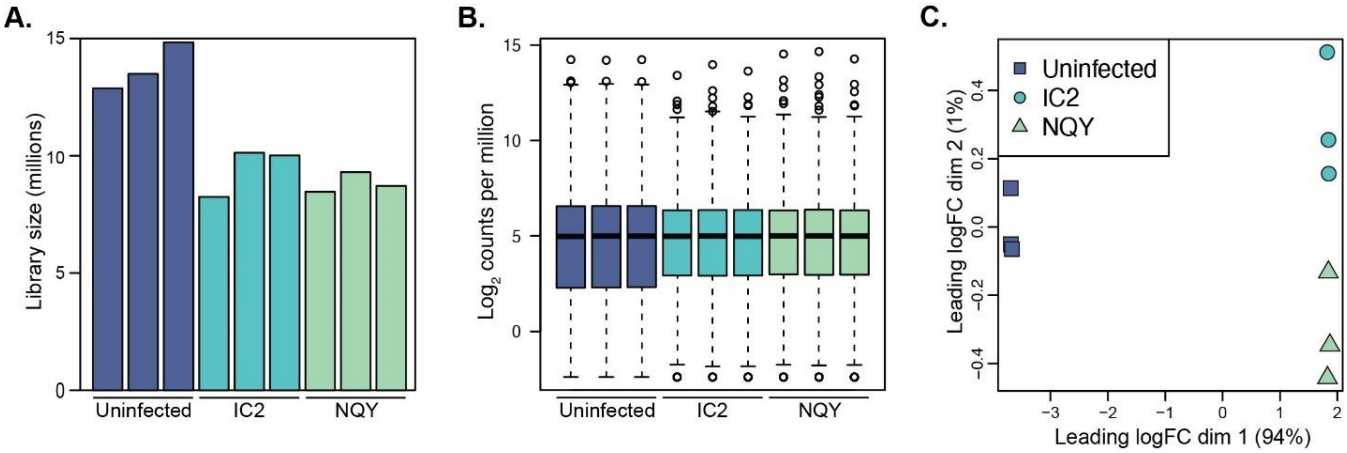

Figure 1. Transcriptional profiling of MCMV-infected dendritic cells. (A) Summary of reads mapped to genes in the mm10 genome from dendritic cells (DCs) mock-infected or infected with either wild-type MCMV (IC2) or the M33**NQY** mutant (n=3 per group). (B) edgeR-normalized library size across samples. (C) Multidimensional scaling plot of the normalized libraries showing the relationships between biological replicates of each condition.

Our analysis of MCMV-infected versus mock-infected dendritic cells revealed massive transcriptional reprogramming, with 2,541 genes showing significant differential expression in wild-type (IC2) infection using stringent criteria ($|\log_2 FC| > 2$ and FDR < 0.05) (Fig. 2A; Table S2). Similarly, the M33NQY mutant virus induced substantial transcriptional changes, with 2,573 genes significantly altered (Fig. 2A, Table S3). Wild-type MCMV infection resulted in 1,883 significantly upregulated and 658 significantly downregulated genes, while M33NQY infection showed comparable effects with 1,905 upregulated and 668 downregulated genes (Fig. 2B).

Both viruses induced similar patterns of extreme gene expression changes, with top upregulated genes in both infections including Emp1 ($\log_2 FC$ = 12.58 in IC2, 12.49 in NQY), Plaur ($\log_2 FC$ = 12.44 in IC2, 12.19 in NQY), and Klf14 ($\log_2 FC$ = 11.35 in IC2, 11.37 in NQY). Both viruses strongly suppressed immune-related genes, including Ptprh ($\log_2 FC$ = -8.66 in both strains), Fgd2 ($\log_2 FC$ = -7.18 in IC2, -7.38 in NQY), and Clec9a ($\log_2 FC$ = -7.04 in IC2, -7.24 in NQY). The downregulation of Clec9a is particularly noteworthy as this C-type lectin receptor is specifically expressed by conventional dendritic cells and is crucial for cross-presentation of necrotic cell-associated antigens to CD8+ T cells (Sancho et al., 2009; Zelenay et al., 2012; Zhang et al., 2012).

The comparison between wild-type (IC2) and M33NQY mutant MCMV-infected dendritic cells revealed far more subtle transcriptional differences. Using less stringent criteria ($|\log_2 FC| > 0.5$ and FDR < 0.05), we identified only 35 significantly differentially expressed genes (Fig. 2C**;** Table S4). Of these, 22 genes were upregulated and 13 genes were downregulated in IC2 compared to NQY-infected cells. The most differentially expressed gene was the lincRNA 2310001H17Rik which is currently uncharacterised ($\log_2 FC$ = 2.18), followed by several immune-related genes, including Ifit1bl1 ($\log_2 FC$ = 1.53), Apol7c ($\log_2 FC$ = 1.37), and the complement component C3 ($\log_2 FC$ = 1.34). Notably, Nos2 (inducible nitric oxide synthase) was downregulated in IC2 compared to NQY-infected cells ($\log_2 FC$ = -1.16), potentially indicating differences in inflammatory response regulation between the two viral strains.

Pathway analysis reveals coordinated targeting of antigen presentation and cell migration processes

KEGG pathway enrichment analysis identified significant (padj < 0.01) downregulation in multiple immune and migration-related pathways in both wild-type and M33NQY mutant infections (Fig. 2D; Tables S4, S5). For wild-type MCMV, the most downregulated pathways included Coronavirus disease (NES = -2.50), B cell receptor signaling pathway (NES = -2.43), Ribosome (NES = -2.40), and Leukocyte transendothelial migration (NES = -2.36). In M33NQY-infected cells, Fc gamma R-mediated phagocytosis ranked first (NES = -2.47), followed by Coronavirus disease (NES = -2.42), Leukocyte transendothelial migration (NES = -2.41), and B cell receptor signaling pathway (NES = -2.40). Antigen processing and presentation were also significantly downregulated in both conditions (NES = -2.26 in IC2, rank #7; NES = -2.27 in NQY, rank #6).

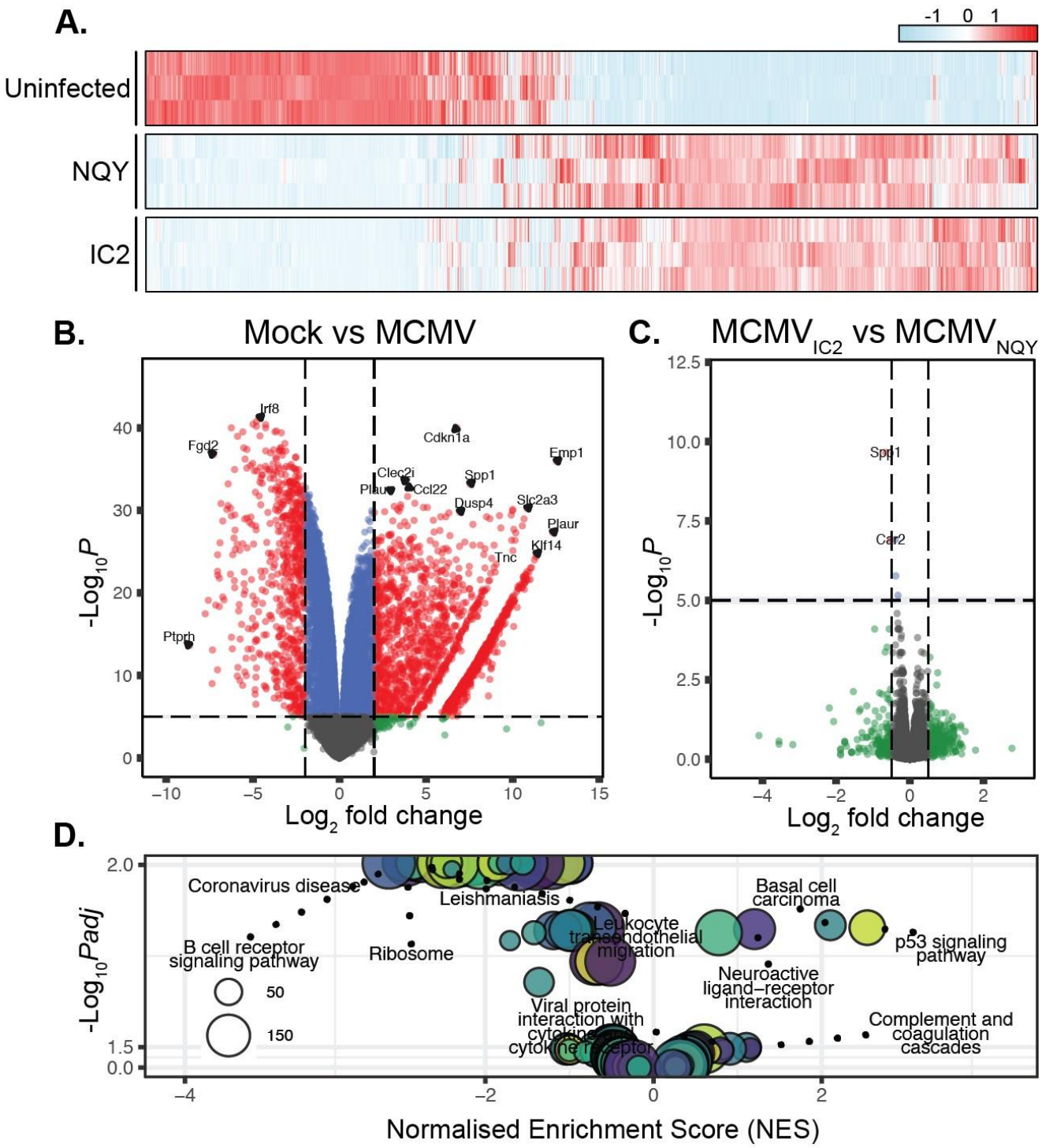

Figure 2. Differential gene expression in MCMV-infected dendritic cells. (A) Heat map of mouse genes with normalised expression values, scaled per gene. B) Volcano plot of differentially expressed genes in wild-type (IC2) MCMV-infected DCs compared to mock controls. Red: significantly differentially expressed genes ($|\log_2 FC| > 2$, FDR < 0.05); Blue: significant genes not meeting fold change cutoff; Gray: non-significant genes; Green: genes not passing FDR threshold. Selected immune-related genes are labeled. Only genes that had a collective minimum count >10 were used, n=12805 genes. (C) Volcano plot depicting differential gene expression between DCs infected with wild-type MCMV (IC2) and the M33NQY mutant. (D) Functional enrichment analysis showing significantly enriched KEGG pathways. Bubble size corresponds to gene count with statistical significance on the y-axis and

normalized enrichment score on the x-axis. The top 5 and bottom five NES score hits are individually labelled. Bubble colour is arbitrarily chosen to discriminate bubbles.

We also observed significant upregulation (padj < 0.05) of several pathways. The p53 signaling pathway showed the highest positive enrichment in both infections (NES = 2.22 in IC2; NES = 2.26 in NQY), suggesting activation of stress response mechanisms. Other upregulated pathways included Complement and coagulation cascades (NES = 1.70 in IC2; NES = 1.72 in NQY), Viral protein interaction with cytokine and cytokine receptor (NES = 1.68 in IC2; NES = 1.67 in NQY), and Cytokine-cytokine receptor interaction (NES = 1.58 in IC2; NES = 1.61 in NQY).

Gene Ontology biological process analysis further supported these findings, with significant downregulation in terms related to antigen processing and presentation (GO:0019882, NES = -2.63 in IC2, -2.62 in NQY), T cell activation (GO:0042110, NES = -2.41 in IC2, -2.39 in NQY), and leukocyte migration (GO:0050900, NES = -2.29 in IC2, -2.26 in NQY). Broader immune system processes were also suppressed in both infections, including leukocyte activation (NES = -2.35 in IC2, -2.33 in NQY) and regulation of immune system process (NES = -2.24 in IC2, -2.30 in NQY). Both viruses showed significant upregulation of biological processes related to DNA metabolism (NES = 2.68 in IC2, 2.73 in NQY), DNA replication (NES = 2.65 in IC2, 2.68 in NQY), and cell cycle processes (NES = 2.46 in IC2, 2.52 in NQY), likely reflecting viral hijacking of host cellular machinery to support MCMV genome replication.

Comparing wild-type MCMV and M33NQY mutant MCMV transcriptional effects

KEGG pathway analysis comparing WT MCMV (IC2) versus the M33NQY mutant revealed a selective pattern of enrichment with a distinct emphasis on cell migration and cytoskeletal organization pathways (Table S6). Leukocyte transendothelial migration showed the strongest positive enrichment (NES = 2.11, padj < 0.05), followed by Fc gamma R-mediated phagocytosis (NES = 2.09, padj < 0.05), Focal adhesion (NES = 2.05, padj < 0.05), and Regulation of actin cytoskeleton (NES = 1.97, padj < 0.05). These findings align with previous work demonstrating M33's critical role in DC migration and dissemination (Farrell et al., 2017; Ma et al., 2022).

While the comparison between wild-type and M33NQY mutant revealed relatively subtle transcriptional differences (only 35 genes with $|\log_2 FC| > 0.5$ and FDR < 0.05, Fig. 2C), we identified significant changes in key migration-related molecules. The most statistically significant difference was observed in Spp1 (osteopontin, $\log_2 FC = 0.65$, FDR < 1e-9), a secreted glycoprotein critical for leukocyte migration and DC maturation (Renkl et al., 2005). Other significantly upregulated migration-related genes in wild-type MCMV included cytoskeletal components (Actg1, $\log_2 FC = 0.26$, FDR < 0.0001; Actb, $\log_2 FC = 0.19$, FDR < 0.002), cell adhesion and matrix interaction factors (Tnc, $\log_2 FC = 0.56$, FDR < 0.0001; Plau, $\log_2 FC = 0.39$, FDR < 1e-7), cytoskeletal regulators (Gsn, $\log_2 FC = 0.32$, FDR < 0.0001; Rac2, $\log_2 FC = 0.18$, FDR < 0.01), and adhesion proteins (Icam1, $\log_2 FC = 0.17$, FDR < 0.03). Notably, Car2 ($\log_2 FC = 0.52$, FDR < 1e-7) was also significantly upregulated, suggesting potential involvement of pH regulation mechanisms. The lincRNA 2310001H17Rik ($\log_2 FC = 2.18$, FDR < 0.03) showed the largest fold change, followed by the interferon-inducible gene Ifit1bl1 ($\log_2 FC = 1.53$, FDR < 0.01) and complement component C3 ($\log_2 FC = 1.34$, FDR < 0.03), suggesting additional

regulatory mechanisms. Similar upregulation of migration-associated genes has been observed in HCMV-infected endothelial cells expressing the homologous US28 vGPCR (Maussang et al., 2009; Vomaske et al., 2009).

Downregulated pathways in the wild-type versus M33NQY comparison were primarily related to ribosomal functions and metabolic processes, with Ribosome showing the strongest negative enrichment (NES = -2.29, padj < 0.05). Antigen processing and presentation pathways showed no significant differences between wild-type and M33NQY infections (NES = -1.25, padj > 0.25), suggesting that M33 signaling selectively enhances migration without affecting MCMV's immune evasion mechanisms.

MCMV systematically targets the MHC class II antigen presentation pathway

Our transcriptomic analysis revealed coordinated downregulation across multiple components of the MHC class II antigen presentation pathway in MCMV-infected dendritic cells (Fig. 3A), consistent with previous observations of MHC class II suppression by cytomegaloviruses (Lee et al., 2011; Tomazin et al., 1999; Yunis et al., 2018). The core MHC class II molecules showed profound downregulation in both wild-type and M33NQY mutant infections, with H2-Aa (log_2FC = -4.77 in IC2; -4.82 in NQY), H2-Ab1 (log_2FC = -4.99 in both strains), and H2-Eb1 (log_2FC = -4.32 in IC2; -4.20 in NQY) all showing significant reduction. Peptide-loading machinery components were similarly suppressed, including H2-DMa (log_2FC = -5.55 in IC2; -5.36 in NQY), H2-DMb1 (log_2FC = -4.54 in IC2; -4.44 in NQY), H2-DMb2 (log_2FC = -7.58 in IC2; -6.22 in NQY), and H2-Ob (log_2FC = -2.90 in IC2; -2.51 in NQY).

Most notably, the Class II Transactivator (CIITA), the master regulator of MHC class II expression, showed substantial downregulation (log_2FC = -6.45 in IC2; -7.03 in NQY), as did the invariant chain CD74 (log_2FC = -5.49 in IC2; -6.02 in NQY), which plays multiple roles in MHC class II trafficking and peptide loading. This targeting of CIITA is reminiscent of the strategy employed by HCMV, which inhibits IFN-γ-induced upregulation of CIITA in infected cells (Le Roy et al., 1999; Lee et al., 2011).Transcriptional regulators of MHC class II expression showed varied responses, with Rfx5 downregulated (log_2FC = -1.26 in IC2; -1.30 in NQY), while Rfxank (log_2FC = 0.28 in IC2; 0.36 in NQY) and Rfxap (log_2FC = 0.17 in IC2; 0.24 in NQY) showed modest upregulation.

The overall pattern of comprehensive MHC class II pathway downregulation was conserved between both viral strains, suggesting this immune evasion strategy operates independently of M33 signaling.

MCMV modulates leukocyte migration pathways and NQY has reduced leukocyte migration.

Our GSEA identified the KEGG Leukocyte Transendothelial Migration pathway as significantly altered in MCMV-infected DCs. Heatmap visualization of the leading-edge genes from this pathway (Fig. 3B) demonstrates altered expression in both IC2 and NQY-infected cells, though with distinct patterns between the two viral strains.Integrins showed mixed regulation patterns,

with ITGB1 upregulated ($log_2FC = 0.86$) while ITGB2 was significantly downregulated ($log_2FC = -1.43$), suggesting selective modulation of specific adhesion pathways.

Cytoskeletal regulators, critical for DC migration, showed substantial alterations. The actin cytoskeleton components ACTB ($log_2FC = 0.92$) and ACTG1 ($log_2FC = 0.88$) were upregulated, while key regulators of cytoskeletal dynamics including RAC1 ($log_2FC = 0.76$) and RAC2 ($log_2FC = 0.68$) also showed increased expression. These Rho GTPases serve as molecular switches that coordinate the cytoskeletal remodeling necessary for cell migration.

Signaling molecules governing directional migration exhibited altered expression patterns, with PI3K components showing mixed regulation (PIK3CD, $log_2FC = 1.14$; PIK3R1, $log_2FC = -0.83$; PIK3R2, altered in both infections). The ERM (ezrin-radixin-moesin) family proteins, which link plasma membrane proteins to the actin cytoskeleton, were also modulated, with MSN and EZR showing differential expression between IC2 and NQY infections.

Many migration-related genes show stronger expression in IC2-infected cells than NQY-infected cells (Fig 3B), suggesting that functional M33 signaling enhances expression of specific migration-related genes, consistent with the known role of M33 in promoting DC migration during MCMV infection.

Integrated network analysis of antigen presentation and leukocyte migration.

Network analysis of the leading-edge genes from the KEGG Antigen Processing and Presentation and Leukocyte Transendothelial Migration pathways revealed key regulatory nodes connecting these components (Fig. 3C). The network visualization demonstrated extensive interconnectivity between antigen presentation machinery components and leukocyte migration regulators, with several hub genes exhibiting high betweenness centrality values.

B2m (beta-2-microglobulin) emerged as the most critical hub gene in the network, displaying the highest betweenness centrality. While primarily known as an essential component of MHC class I molecules, B2m showed significant downregulation in MCMV-infected DCs, potentially affecting both antigen presentation and cell adhesion processes. Three additional major hub genes—Itgb1 (integrin subunit beta 1), Itgam (integrin alpha M, CD11b), and Icam1 (intercellular adhesion molecule 1)—formed a highly interconnected cluster at the interface of immune recognition and cellular migration pathways. Itgb1, which mediates cell-cell and cell-matrix interactions essential for leukocyte trafficking, showed moderate upregulation in MCMV infection. Similarly, Icam1, a critical endothelial adhesion molecule facilitating leukocyte transendothelial migration, displayed increased expression particularly in wild-type MCMV compared to M33NQY infection.

The network analysis also identified significant secondary hubs, including Rho GTPases (Rac1, Rhoa, Cdc42) and cytoskeletal components (Actb, Actg1), which coordinate the cellular machinery required for MHC trafficking and DC motility. These interconnected nodes represent potential convergence points where MCMV can simultaneously modulate antigen presentation and migration capabilities of infected dendritic cells.

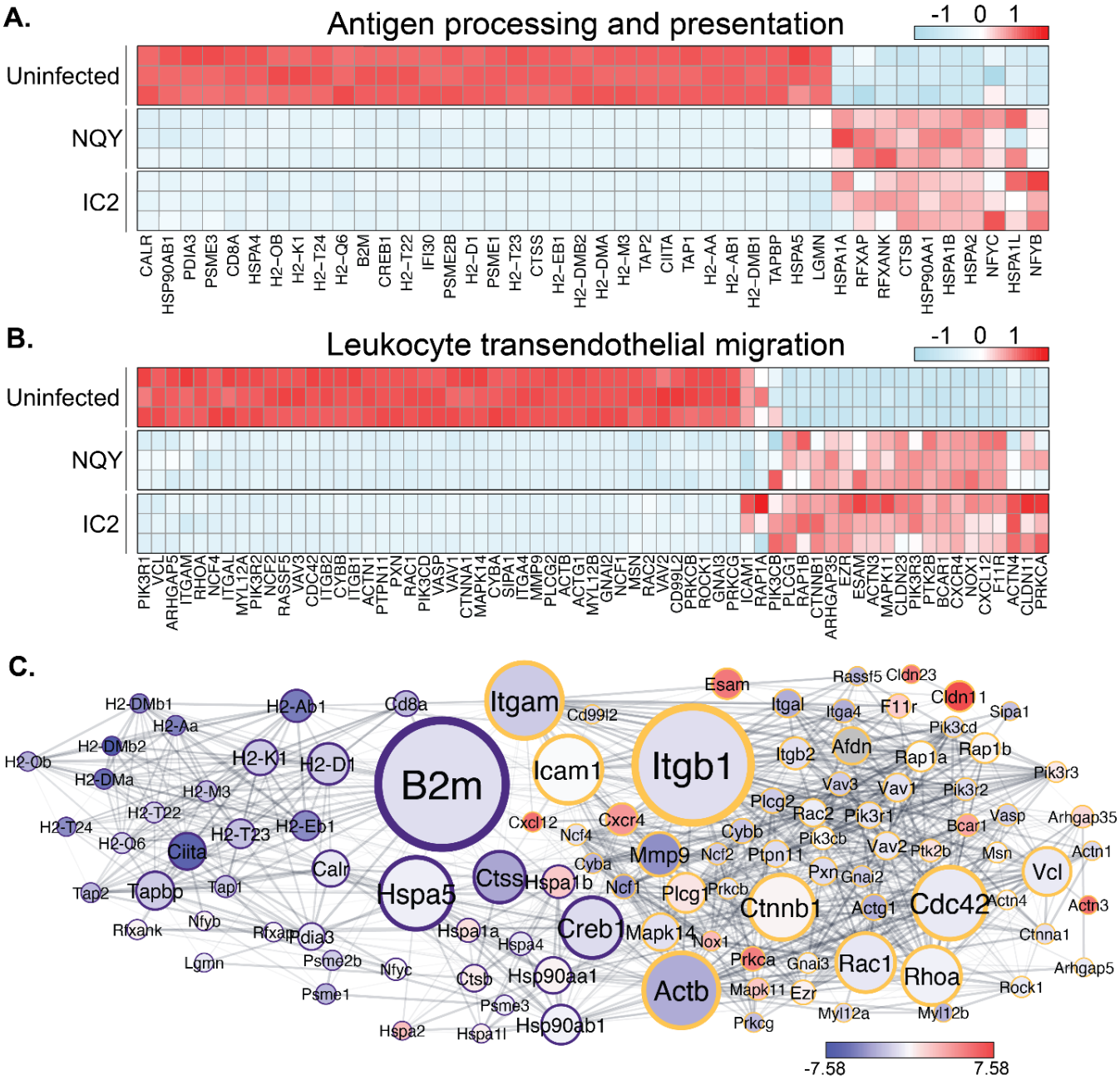

Figure 3. MCMV infection downregulates MHC class II antigen presentation machinery and leukocyte migration in dendritic cells. Heatmap of leading-edge genes from the (A) KEGG Antigen Processing and Presentation pathway or (B) KEGG Leukocyte Transendothelial Migration pathway across experimental conditions. For both heatmaps, each column represents a gene and each row represents a biological replicate. The color scale indicates normalized expression values (C) Network analysis of differentially expressed genes involved in antigen presentation and leukocyte migration pathways. Purple rings: genes in antigen presentation pathway; Yellow rings: genes in leukocyte migration pathway. Node size represents betweenness centrality, node colour indicates $\log_2$FC, and edge thickness corresponds to STRING interaction confidence score.

MCMV gene expression patterns in infected dendritic cells

Our RNA-seq analysis of MCMV-infected dendritic cells at 48 hours post-infection revealed robust expression of MCMV genes across all temporal classes of viral genes, indicating productive infection (Fig. 4A). The viral transcriptome included high expression of immune evasion genes (m04, m06, m152, m144, m157), chemokine and cytokine modulators (m131/129, m133, m145), and tegument proteins including pp71 (M82). Multidimensional scaling analysis demonstrated clear clustering of biological replicates for both virus strains (Fig. 4B).

The vGPCR M33 showed comparable expression levels in both wild-type and NQY mutant infections, confirming that observed phenotypic differences stem from the signaling defect rather than altered gene expression. Comparison of viral gene expression profiles revealed largely similar patterns across the viral genome (Fig. 4C). Only the M57 gene, which encodes the viral major capsid protein, showed modestly higher expression in the M33NQY mutant compared to wild-type virus ($\log_2$FC = 0.58, FDR < 0.05).

This minimal difference in viral gene expression supports our conclusion that the observed phenotypic and host transcriptional differences between wild-type and M33NQY infections stem specifically from the M33 signaling defect rather than from alterations in the viral transcriptional program.

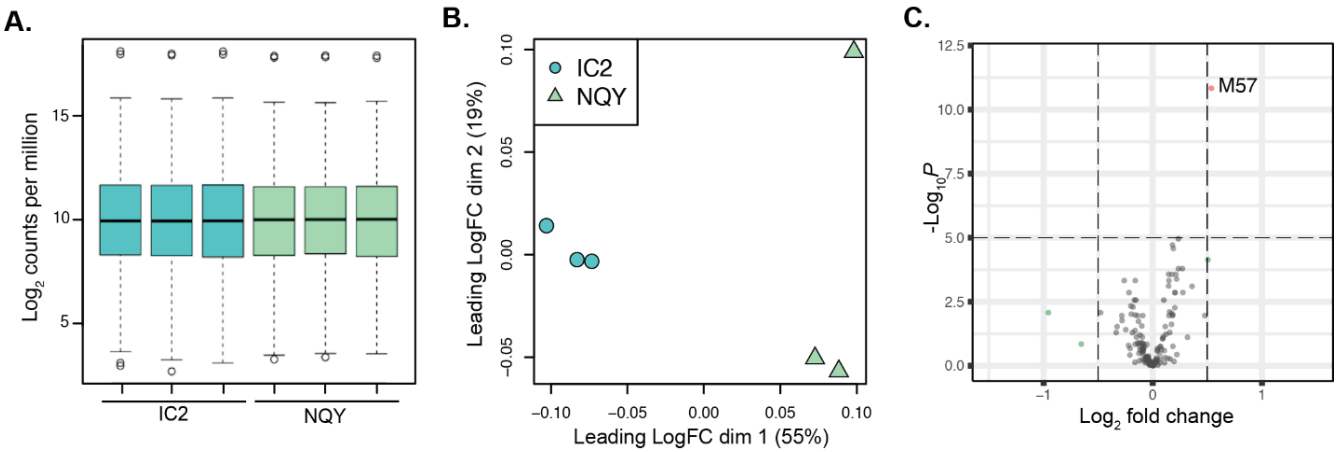

Figure 4. Transcriptional expression of the MCMV genome. (A) Boxplot of normalized MCMV genes per library. (B) Multidimensional scaling plot showing relationships between biological replicates of IC2-infected and M33NQY-infected DCs.(C) Volcano plot of differentially expressed MCMV genes between wild-type and M33NQY-infected DCs. Red: significantly differentially expressed genes ($|\log_2 FC| > 0.5$, FDR < 0.05); Blue: significant genes not meeting fold change cutoff; Gray: non-significant genes; Green: genes not passing FDR threshold, n=159 MCMV genes.

Discussion:

Our global transcriptional analysis of MCMV-infected dendritic cells reveals a sophisticated viral strategy that simultaneously impairs antigen presentation while selectively enhancing migration capabilities, facilitating viral dissemination and evading immune detection. Three key findings

emerge from our data: (1) MCMV systematically downregulates the entire MHC class II antigen presentation machinery, (2) M33 signaling specifically enhances the expression of genes involved in transendothelial migration, and (3) these dual mechanisms operate largely independently, with M33 having minimal impact on MHC class II suppression.

The coordinated downregulation of multiple MHC class II pathway components represents a comprehensive immune evasion strategy that targets a central adaptive immunity mechanism. The particularly strong suppression of CIITA ($\log_2$FC > -6.4), the master transcriptional regulator of MHC class II genes, suggests this represents a strategic viral target rather than a nonspecific effect of infection, consistent with HCMV infected CD34(+) dendritic cells (Lee et al., 2011). By targeting CIITA, MCMV can simultaneously suppress multiple MHC class II machinery components through a single regulatory node. This finding extends previous observations in HCMV-infected monocytes, where MHC II and CD74 transcripts were diminished, demonstrating a more comprehensive suppression in actively infected DCs across the entire antigen presentation pathway. This represents a significant evolutionary adaptation, allowing MCMV to shield itself from CD4+ T cell recognition precisely within the specialized cells for initiating these responses.

Our comparative analysis between wild-type and M33NQY MCMV revealed the specific contribution of M33 signaling to the enhancement of DC migration capabilities. While the overall transcriptional differences were subtle (only 35 genes with $|\log_2\text{FC}| > 0.5$ and FDR < 0.05), the most statistically significant changes occurred in genes critical for cell migration. Most notably, Spp1 (osteopontin, $\log_2$FC = 0.65, FDR < 1e-9), a secreted glycoprotein essential for leukocyte migration and DC maturation, showed the highest statistical significance of all differentially expressed genes. Given its role in both DC maturation and motility, the marked M33-dependent upregulation of Spp1 likely contributes directly to the enhanced tissue dissemination observed *in vivo*. The M33-dependent upregulation of cytoskeletal components (Actg1, $\log_2$FC = 0.26, FDR < 0.0001; Actb, $\log_2$FC = 0.19, FDR < 0.002), cell adhesion and matrix interaction factors (Tnc, $\log_2$FC = 0.56, FDR < 0.0001; Plau, $\log_2$FC = 0.39, FDR < 1e-7), and adhesion molecules (Icam1, $\log_2$FC = 0.17, FDR < 0.03) provides the molecular basis for previously observed defects in lymph node escape by M33NQY-infected DCs (Ma et al., 2022). This remarkable specificity of M33's effects—enhancing migration pathways without substantially affecting viral gene expression or immune evasion mechanisms—indicates this vGPCR has evolved to modulate discrete host cellular functions that benefit viral dissemination.

Our network analysis revealed critical regulatory nodes bridging antigen presentation and migration pathways, with B2m emerging as the most central hub gene. The prominent position of B2m in our network suggests MCMV's modulation of this MHC class I component may have broader implications beyond CD8+ T cell evasion, potentially affecting cell adhesion and migration processes (Farrell et al., 2019). Functional studies have demonstrated that B2m can act beyond its classical role in MHC class I presentation, directly regulating cell adhesion and migration through interaction with integrin signaling pathways (Huang et al., 2008). This broader signaling role of B2m may explain its position as a central hub connecting antigen presentation and migration networks in our analysis

The identification of Itgb1, Itgam, and Icam1 as major secondary hubs demonstrates the interconnected nature of immune recognition and cellular migration, providing molecular targets through which MCMV can efficiently coordinate its dual-modulation strategy. The cytoskeletal regulatory components, including Rac1, Rhoa, and Cdc42, further highlight convergence points where viral manipulation can simultaneously impact both antigen presentation and migration capabilities. Notably, the human cytomegalovirus (HCMV) vGPCR encoded by US28, which possesses a signalling profile similar to M33 (Waldhoer et al., 2002) also converges with the RhoA GTPase signal transduction pathway (Melnychuk et al., 2004) important for cellular migration, suggesting conserved functionality.

Our findings have broader implications for understanding betaherpesvirus pathogenesis and host-pathogen interactions. The identification of M33 as a specific enhancer of migration-related pathways, rather than a general regulator of viral gene expression, highlights how viral proteins can evolve specialised functions that appropriate normal cellular processes (White et al., 2022). The systematic targeting of the MHC class II pathway, particularly through CIITA suppression, reveals a strategic viral approach to immune evasion that maximizes effectiveness while minimizing the genetic investment required.

The strong association of Spp1 with M33-dependent migration enhancement presents a particularly intriguing target for potential intervention. As the most significantly differentially expressed gene between wild-type and M33NQY-infected cells, osteopontin likely plays a central role in facilitating the enhanced migratory capabilities of MCMV-infected DCs. The importance of this glycoprotein in both migration and DC maturation suggests it could serve as a valuable biomarker or therapeutic target specific to the viral dissemination phase. Targeting Spp1 or its downstream effectors might provide a strategy to limit viral spread while minimizing disruption to normal immune functions (Icer and Gezmen-Karadag, 2018).

This transcriptomic analysis provides a molecular roadmap of how MCMV manipulates dendritic cell biology to facilitate dissemination. By identifying specific pathways and regulatory nodes targeted by viral mechanisms, our findings highlight potential intervention points for preventing viral dissemination and enhancing immune recognition of infected cells. The central role of B2m, Itgb1, Itgam, and Icam1 in connecting immune and migration networks suggests these molecules might represent valuable targets for therapeutic intervention. Future studies should focus on elucidating the specific viral factors responsible for CIITA suppression and determining how M33 signaling selectively enhances migration-related gene expression through these key regulatory nodes.

Data availability

RNA sequencing data generated for this study have been deposited in the NCBI Sequence Read Archive (SRA), available under accession number PRJNA1071051. Count data for mouse and MCMV genes and R scripts are available via GitHub at github.com/rhparry/MCMV_transcriptome/

Acknowledgements

This work utilised the Australian Galaxy service (https://usegalaxy.org.au/). We acknowledge

resources prepared by Dr. Andrii Slonchak for help with Cytoscape analysis, visualisation and interpretation.

Author contributions

H.E.F conceived the study. K.B. and H.E.F collected the primary samples. H.E.F obtained funding. R.H.P and C.L.D.M performed the analyses. R.H.P and C.L.D.M provided visualisation. R.H.P., C.LD.M, and H.E.F drafted the manuscript. H.E.F provided resources. All authors reviewed and edited the manuscript.

Funding information

These studies were funded by the National Health and Medical Research Council of Australia (1140169), the Australian Research Council (DP190101851) and Queensland Health. The funders had no role in the study design, data collection, data interpretation or the decision to submit the work for publication.

SUPPLEMENTARY INFORMATION

Supplementary Table 1: mRNA sequencing sample metrics

Sample	Reads	Mapped to mm10	%	Mapped to MCMV	%	SRA accession
Mock 1	15717275	15285050	97.25	0	0	SRR27781981
Mock 2	16626913	16179649	97.31	0	0	SRR27781980
Mock 3	18448704	17933985	97.21	0	0	SRR27781979
IC2 1	12935375	9797253	75.74	2405980	18.6	SRR27781978
IC2 2	16133113	12224060	75.77	2953973	18.31	SRR27781977
IC2 3	15779248	11978027	75.91	2916005	18.48	SRR27781976
NQY 1	13630492	10457313	76.72	2326725	17.07	SRR27781975
NQY 2	14810367	11460262	77.38	2520724	17.02	SRR27781974
NQY 3	13841341	10601083	76.59	2401473	17.35	SRR27781973

- Table S2: Differentially expressed genes in wild-type (IC2) MCMV infected cells compared to Mock.
- Table S3: Differentially expressed genes in M33NQY MCMV infection compared to Mock.
- Table S4: Differentially expressed genes between MCMV-IC2-infected versus MCMV-NQY-infected cells
- Table S5: easyGSEA results of wild-type (IC2) MCMV infected cells compared to Mock.
- Table S6: easyGSEA results in M33NQY MCMV infected cells compared to Mock.
- Table S7: easyGSEA results in MCMV-IC2-infected versus MCMV-NQY-infected cells.

References

Allavena, P., Sica, A., Vecchi, A., Locati, M., Sozzani, S., Mantovani, A., 2000. The chemokine receptor switch paradigm and dendritic cell migration: its significance in tumor tissues. Immunol Rev 177, 141-149.

Andrews, D.M., Andoniou, C.E., Granucci, F., Ricciardi-Castagnoli, P., Degli-Esposti, M.A., 2001. Infection of dendritic cells by murine cytomegalovirus induces functional paralysis. Nat Immunol 2, 1077-1084.

Auffermann-Gretzinger, S., Keeffe, E.B., Levy, S., 2001. Impaired dendritic cell maturation in patients with chronic, but not resolved, hepatitis C virus infection. Blood 97, 3171-3176.

Bajenoff, M., Egen, J.G., Koo, L.Y., Laugier, J.P., Brau, F., Glaichenhaus, N., Germain, R.N., 2006. Stromal cell networks regulate lymphocyte entry, migration, and territoriality in lymph nodes. Immunity 25, 989-1001.

Banchereau, J., Steinman, R.M., 1998. Dendritic cells and the control of immunity. Nature 392, 245-252.

Boeckh, M., Geballe, A.P., 2011. Cytomegalovirus: pathogen, paradigm, and puzzle. J Clin Invest 121, 1673-1680.

Bruce, K., Ma, J., Lawler, C., Xie, W., Stevenson, P.G., Farrell, H.E., 2022. Recent Advancements in Understanding Primary Cytomegalovirus Infection in a Mouse Model. Viruses 14.

Cardin, R.D., Schaefer, G.C., Allen, J.R., Davis-Poynter, N.J., Farrell, H.E., 2009. The M33 chemokine receptor homolog of murine cytomegalovirus exhibits a differential tissue-specific role during in vivo replication and latency. J Virol 83, 7590-7601.

Cheng, X., Yan, J., Liu, Y., Wang, J., Taubert, S., 2021. eVITTA: a web-based visualization and inference toolbox for transcriptome analysis. Nucleic Acids Res 49, W207-W215.

Davis-Poynter, N.J., Lynch, D.M., Vally, H., Shellam, G.R., Rawlinson, W.D., Barrell, B.G., Farrell, H.E., 1997. Identification and characterization of a G protein-coupled receptor homolog encoded by murine cytomegalovirus. J Virol 71, 1521-1529.

Farrell, H.E., Bruce, K., Lawler, C., Oliveira, M., Cardin, R., Davis-Poynter, N., Stevenson, P.G., 2017. Murine Cytomegalovirus Spreads by Dendritic Cell Recirculation. mBio 8.

Farrell, H.E., Bruce, K., Lawler, C., Stevenson, P.G., 2019. Murine Cytomegalovirus Spread Depends on the Infected Myeloid Cell Type. J Virol 93.

Farrell, H.E., Lawler, C., Oliveira, M.T., Davis-Poynter, N., Stevenson, P.G., 2015. Alveolar Macrophages Are a Prominent but Nonessential Target for Murine Cytomegalovirus Infecting the Lungs. J Virol 90, 2756-2766.

Farrell, H.E., Lawler, C., Tan, C.S., MacDonald, K., Bruce, K., Mach, M., Davis-Poynter, N., Stevenson, P.G., 2016. Murine Cytomegalovirus Exploits Olfaction To Enter New Hosts. mBio 7, e00251-00216.

Forster, R., Davalos-Misslitz, A.C., Rot, A., 2008. CCR7 and its ligands: balancing immunity and tolerance. Nat Rev Immunol 8, 362-371.

Garg, S., Oran, A., Wajchman, J., Sasaki, S., Maris, C.H., Kapp, J.A., Jacob, J., 2003. Genetic tagging shows increased frequency and longevity of antigen-presenting, skin-derived dendritic cells in vivo. Nat Immunol 4, 907-912.

Griffiths, P., Baraniak, I., Reeves, M., 2015. The pathogenesis of human cytomegalovirus. J Pathol 235, 288-297.

Guermonprez, P., Valladeau, J., Zitvogel, L., Thery, C., Amigorena, S., 2002. Antigen presentation and T cell stimulation by dendritic cells. Annu Rev Immunol 20, 621-667.

Huang, W.C., Havel, J.J., Zhau, H.E., Qian, W.P., Lue, H.W., Chu, C.Y., Nomura, T., Chung, L.W., 2008. Beta2-microglobulin signaling blockade inhibited androgen receptor axis and caused apoptosis in human prostate cancer cells. Clin Cancer Res 14, 5341-5347.

Icer, M.A., Gezmen-Karadag, M., 2018. The multiple functions and mechanisms of osteopontin. Clin Biochem 59, 17-24.

Ingulli, E., Mondino, A., Khoruts, A., Jenkins, M.K., 1997. In vivo detection of dendritic cell antigen presentation to CD4(+) T cells. J Exp Med 185, 2133-2141.

Iwasaki, A., 2007. Mucosal dendritic cells. Annu Rev Immunol 25, 381-418.

Kamath, A.T., Henri, S., Battye, F., Tough, D.F., Shortman, K., 2002. Developmental kinetics and lifespan of dendritic cells in mouse lymphoid organs. Blood 100, 1734-1741.

Krmpotic, A., Bubic, I., Polic, B., Lucin, P., Jonjic, S., 2003. Pathogenesis of murine cytomegalovirus infection. Microbes Infect 5, 1263-1277.

Le Roy, E., Muhlethaler-Mottet, A., Davrinche, C., Mach, B., Davignon, J.L., 1999. Escape of human cytomegalovirus from HLA-DR-restricted CD4(+) T-cell response is mediated by repression of gamma interferon-induced class II transactivator expression. J Virol 73, 6582-6589.

Lee, A.W., Wang, N., Hornell, T.M., Harding, J.J., Deshpande, C., Hertel, L., Lacaille, V., Pashine, A., Macaubas, C., Mocarski, E.S., Mellins, E.D., 2011. Human cytomegalovirus decreases constitutive transcription of MHC class II genes in mature Langerhans cells by reducing CIITA transcript levels. Mol Immunol 48, 1160-1167.

Lemmermann, N.A., Bohm, V., Holtappels, R., Reddehase, M.J., 2011. In vivo impact of cytomegalovirus evasion of CD8 T-cell immunity: facts and thoughts based on murine models. Virus Res 157, 161-174.

Loewendorf, A., Benedict, C.A., 2010. Modulation of host innate and adaptive immune defenses by cytomegalovirus: timing is everything. J Intern Med 267, 483-501.

Luber, C.A., Cox, J., Lauterbach, H., Fancke, B., Selbach, M., Tschopp, J., Akira, S., Wiegand, M., Hochrein, H., O'Keeffe, M., Mann, M., 2010. Quantitative proteomics reveals subset-specific viral recognition in dendritic cells. Immunity 32, 279-289.

Ma, J., Bruce, K., Davis-Poynter, N., Stevenson, P.G., Farrell, H.E., 2022. The Mouse Cytomegalovirus G Protein-Coupled Receptor Homolog, M33, Coordinates Key Features of In Vivo Infection via Distinct Components of Its Signaling Repertoire. J Virol 96, e0186721.

Ma, J., Bruce, K., Stevenson, P.G., Farrell, H.E., 2021. Murine Cytomegalovirus MCK-2 Facilitates In Vivo Infection Transfer from Dendritic Cells to Salivary Gland Acinar Cells. J Virol 95, e0069321.

Mathys, S., Schroeder, T., Ellwart, J., Koszinowski, U.H., Messerle, M., Just, U., 2003. Dendritic cells under influence of mouse cytomegalovirus have a physiologic dual role: to initiate and to restrict T cell activation. J Infect Dis 187, 988-999.

Maussang, D., Langemeijer, E., Fitzsimons, C.P., Stigter-van Walsum, M., Dijkman, R., Borg, M.K., Slinger, E., Schreiber, A., Michel, D., Tensen, C.P., van Dongen, G.A., Leurs, R., Smit, M.J., 2009. The human cytomegalovirus-encoded chemokine receptor US28 promotes angiogenesis and tumor formation via cyclooxygenase-2. Cancer Res 69, 2861-2869.

Melnychuk, R.M., Streblow, D.N., Smith, P.P., Hirsch, A.J., Pancheva, D., Nelson, J.A., 2004. Human cytomegalovirus-encoded G protein-coupled receptor US28 mediates smooth muscle cell migration through Galpha12. J Virol 78, 8382-8391.

Merad, M., Sathe, P., Helft, J., Miller, J., Mortha, A., 2013. The dendritic cell lineage: ontogeny and function of dendritic cells and their subsets in the steady state and the inflamed setting. Annu Rev Immunol 31, 563-604.
Miller, J.C., Brown, B.D., Shay, T., Gautier, E.L., Jojic, V., Cohain, A., Pandey, G., Leboeuf, M., Elpek, K.G., Helft, J., Hashimoto, D., Chow, A., Price, J., Greter, M., Bogunovic, M., Bellemare-Pelletier, A., Frenette, P.S., Randolph, G.J., Turley, S.J., Merad, M., Immunological Genome, C., 2012. Deciphering the transcriptional network of the dendritic cell lineage. Nat Immunol 13, 888-899.
Randolph, G.J., Angeli, V., Swartz, M.A., 2005. Dendritic-cell trafficking to lymph nodes through lymphatic vessels. Nat Rev Immunol 5, 617-628.
Reeves, M.B., Sinclair, J.H., 2013. Circulating dendritic cells isolated from healthy seropositive donors are sites of human cytomegalovirus reactivation in vivo. J Virol 87, 10660-10667.
Reis e Sousa, C., 2006. Dendritic cells in a mature age. Nat Rev Immunol 6, 476-483.
Renkl, A.C., Wussler, J., Ahrens, T., Thoma, K., Kon, S., Uede, T., Martin, S.F., Simon, J.C., Weiss, J.M., 2005. Osteopontin functionally activates dendritic cells and induces their differentiation toward a Th1-polarizing phenotype. Blood 106, 946-955.
Saederup, N., Lin, Y.C., Dairaghi, D.J., Schall, T.J., Mocarski, E.S., 1999. Cytomegalovirus-encoded beta chemokine promotes monocyte-associated viremia in the host. Proc Natl Acad Sci U S A 96, 10881-10886.
Sancho, D., Joffre, O.P., Keller, A.M., Rogers, N.C., Martinez, D., Hernanz-Falcon, P., Rosewell, I., Reis e Sousa, C., 2009. Identification of a dendritic cell receptor that couples sensing of necrosis to immunity. Nature 458, 899-903.
Shnayder, M., Nachshon, A., Rozman, B., Bernshtein, B., Lavi, M., Fein, N., Poole, E., Avdic, S., Blyth, E., Gottlieb, D., Abendroth, A., Slobedman, B., Sinclair, J., Stern-Ginossar, N., Schwartz, M., 2020. Single cell analysis reveals human cytomegalovirus drives latently infected cells towards an anergic-like monocyte state. Elife 9.
Sinclair, J., Sissons, P., 2006. Latency and reactivation of human cytomegalovirus. J Gen Virol 87, 1763-1779.
Sinclair, J.H., Reeves, M.B., 2013. Human cytomegalovirus manipulation of latently infected cells. Viruses 5, 2803-2824.
Sixt, M., Kanazawa, N., Selg, M., Samson, T., Roos, G., Reinhardt, D.P., Pabst, R., Lutz, M.B., Sorokin, L., 2005. The conduit system transports soluble antigens from the afferent lymph to resident dendritic cells in the T cell area of the lymph node. Immunity 22, 19-29.
Sozzani, S., Allavena, P., D'Amico, G., Luini, W., Bianchi, G., Kataura, M., Imai, T., Yoshie, O., Bonecchi, R., Mantovani, A., 1998. Differential regulation of chemokine receptors during dendritic cell maturation: a model for their trafficking properties. J Immunol 161, 1083-1086.
Suvas, S., Rouse, B.T., 2006. Treg control of antimicrobial T cell responses. Curr Opin Immunol 18, 344-348.
Tomazin, R., Boname, J., Hegde, N.R., Lewinsohn, D.M., Altschuler, Y., Jones, T.R., Cresswell, P., Nelson, J.A., Riddell, S.R., Johnson, D.C., 1999. Cytomegalovirus US2 destroys two components of the MHC class II pathway, preventing recognition by CD4+ T cells. Nat Med 5, 1039-1043.
Vomaske, J., Melnychuk, R.M., Smith, P.P., Powell, J., Hall, L., DeFilippis, V., Fruh, K., Smit, M., Schlaepfer, D.D., Nelson, J.A., Streblow, D.N., 2009. Differential ligand binding to a human cytomegalovirus chemokine receptor determines cell type-specific motility. PLoS Pathog 5, e1000304.

Waldhoer, M., Kledal, T.N., Farrell, H., Schwartz, T.W., 2002. Murine cytomegalovirus (CMV) M33 and human CMV US28 receptors exhibit similar constitutive signaling activities. J Virol 76, 8161-8168.

White, T.M., Bonavita, C.M., Stanfield, B.A., Farrell, H.E., Davis-Poynter, N.J., Cardin, R.D., 2022. The CMV-encoded G protein-coupled receptors M33 and US28 play pleiotropic roles in immune evasion and alter host T cell responses. Front Immunol 13, 1047299.

Yunis, J., Farrell, H.E., Bruce, K., Lawler, C., Sidenius, S., Wyer, O., Davis-Poynter, N., Stevenson, P.G., 2018. Murine cytomegalovirus degrades MHC class II to colonize the salivary glands. PLoS Pathog 14, e1006905.

Zelenay, S., Keller, A.M., Whitney, P.G., Schraml, B.U., Deddouche, S., Rogers, N.C., Schulz, O., Sancho, D., Reis e Sousa, C., 2012. The dendritic cell receptor DNGR-1 controls endocytic handling of necrotic cell antigens to favor cross-priming of CTLs in virus-infected mice. J Clin Invest 122, 1615-1627.

Zhang, J.G., Czabotar, P.E., Policheni, A.N., Caminschi, I., Wan, S.S., Kitsoulis, S., Tullett, K.M., Robin, A.Y., Brammananth, R., van Delft, M.F., Lu, J., O'Reilly, L.A., Josefsson, E.C., Kile, B.T., Chin, W.J., Mintern, J.D., Olshina, M.A., Wong, W., Baum, J., Wright, M.D., Huang, D.C., Mohandas, N., Coppel, R.L., Colman, P.M., Nicola, N.A., Shortman, K., Lahoud, M.H., 2012. The dendritic cell receptor Clec9A binds damaged cells via exposed actin filaments. Immunity 36, 646-657.